Athermal Annealing of Silicon

J. Grun, C. K. Manka, C. A. Hoffman, J. R. Meyer, O. J. Glembocki, R. Kaplan, S. B. Qadri, and E. F. Skelton
Naval Research Laboratory, Washington, D.C. 20375

D. Donnelly and B. Covington
Department of Physics, Sam Houston State University, Huntsville, Texas 77341
(Received 13 August 1996)

We demonstrate a new mechanism for annealing silicon that does not involve the direct application of heat as in conventional thermal annealing or pulsed laser annealing. A laser pulse focused to high power on a small surface spot of a neutron-transmutation-doped silicon slab is shown to anneal regions *far outside* the illuminated spot where no heat was directly deposited. Electrical activation of donors throughout the slab was uniform and comparable to that of thermally annealed control samples. We conjecture that the annealing was caused by mechanical energy introduced by the laser pulse. This new method may provide a viable alternative for annealing semiconductors or other materials. [S0031-9007(97)02418-6]

PACS numbers: 81.05.–t, 62.50.+p, 81.20.Zx

Annealing is critical to the production of semiconductor devices. During this process dopants within a semiconductor crystal lattice can move to locations where the dopants become electrically active, i.e., contribute to electrical conduction in the semiconductor. Annealing is also needed to remove structural damage in crystals. Current semiconductor annealing methods are based on thermal processes which are accompanied by diffusion that degrades the definition of device features [1] or causes new problems, such as increased junction leakage [2,3]. This will be a serious obstacle for the production of next-generation ultra-high-density, low-power semiconductor devices.

We report here the experimental demonstration of an entirely new semiconductor annealing method which is much *faster* than thermal annealing and does not involve the direct application of thermal energy. We show that a laser pulse focused to high power on a small surface spot of a neutron-transmutation-doped silicon slab can initiate a process which electrically activates dopants and also removes structural damage induced by the transmutation process in regions *far outside* the laser illuminated spot where no heat was directly deposited. The electrical characteristics of successfully athermally annealed slabs in our experiment are comparable to what is attainable with commercial furnace annealing.

It is important to realize that we are describing a technique different from conventional pulsed laser annealing (PLA) [4]. In PLA a laser pulse focused to relatively low fluence (of order J/cm^2) is used to heat and anneal areas of the wafer directly beneath the laser spot. In our work, a laser pulse focused to a much higher fluence (of order kJ/cm^2) was found to anneal areas far removed from the laser spot.

To demonstrate athermal annealing, $\sim$25 mm $\times$ $\sim$25 mm $\times$ 2 mm thick neutron-transmutation-doped [5] (NTD) Si slabs were doped to a concentration of 10^{15} cm^{-3}. (In our NTD process neutrons from a reactor irradiated the slabs for 110 hours, transmuting ^{30}Si to ^{31}P. The neutron flux was measured to be 1E13 n/cm^2 sec at 0.25–0.5 eV, 6E11 n/cm^2 sec at 0.5–10 eV, and modeled to be $\sim$3E12 n/cm^2 sec at 10 eV to 1 MeV. The process creates a uniform distribution of phosphorus through the entire slab along with point defect densities several orders of magnitude higher than the phosphorus concentration [6,7].) Seven slabs were placed inside a vacuum chamber and irradiated by one or two pulses from a 1.06-μm wavelength, 5-ns FWHM duration, $\sim$10-joule laser pulse focused to a 1-mm diameter spot. After laser irradiation, the samples were analyzed for changes in activation, carrier density, mobility, resistivity, and crystal structure as a function of position across the entire slab and particularly in areas far from the illuminated spot. Electrical measurements were made using a four-point probe, an advanced Hall method [8,9], and far-infrared spectroscopy [10]. Structural changes in the crystal-lattice were measured with x-ray diffraction [11,12], x-ray topography, and Raman spectroscopy [13]. Unannealed and thermally annealed slabs were used as controls. In two out of seven samples we observed excellent annealing, the evidence for which is described below.

Far-infrared spectroscopy provides clear evidence for the activation of donor species. In this technique, the absorbance spectrum from 150 to 500 cm^{-1} of a sample cooled to 5.5 K is measured by a Fourier transform infrared spectrometer (FTIR). Electrically active donors are known to exhibit Lyman absorption lines at $<$800 cm^{-1}, whose strengths are proportional to the concentration of electrically active donors [10]. Figure 1 shows the absorbance spectra of unannealed, thermally annealed, and two athermally processed slabs. As expected, the spectrum of the unannealed sample shows no Lyman lines because the phosphorus is not electrically active. In contrast, both athermally annealed slabs show distinctive phosphorus Lyman lines up to the 5*p* line. The widths of the lines are

 0031-9007/97/78(8)/1584(4)$10.00

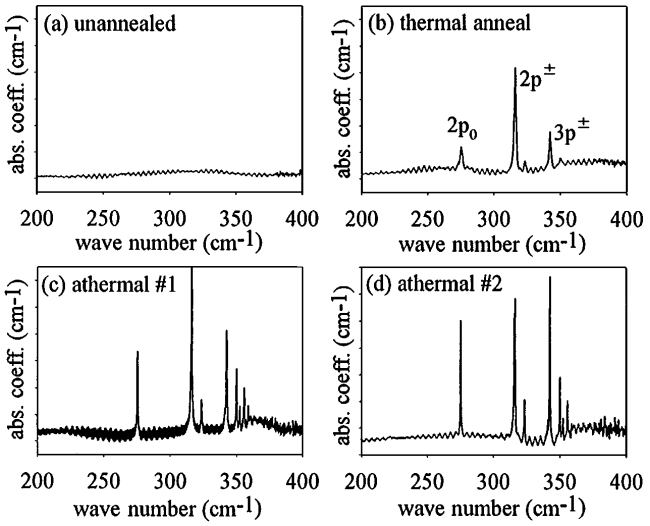

FIG. 1. FTIR absorption spectra, with 1-cm spatial resolution, showing activation of *P* donors by annealing. Shown are spectra from (a) an unannealed NTD Si:P slab, (b) a thermally annealed sample (1 hour at 900 °C in a nitrogen atmosphere), and (c) and (d) athermally annealed, with a 10-joule laser pulse, NTD samples. Integrated areas under a Lorentzian fit to the $2p^{\pm}$ line indicate comparable levels of activation in (b)–(d). The apparent split in the $2p^{\pm}$ line in (d) is noise. Other measurements on these same samples are shown in Figs. 2 and 3 below and described in the text.

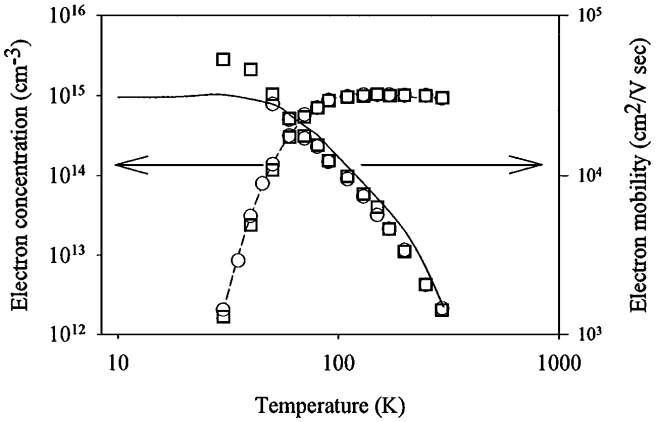

FIG. 2. Hall measurements confirming electrical activation of athermally annealed NTD Si:P slabs. The symbols ○ and □ refer to two different samples. Electron concentration is shown on the left axis. A fit of the standard freeze-out relation to the dashed data curve implies 1.1×10^{15} cm^{-3} activated donors with a binding energy of 43 meV. Electron mobility is shown on the right axis. The solid curve is the mobility for a melt-grown Si:P wafer (Ref. [15]) with donor density of 9.6×10^{14} cm^{-3} and acceptor density of 2.0×10^{14} cm^{-3}. Higher mobilities of athermally annealed slabs at <40 K imply lower compensation.

on the order of 0.55 cm^{-1} (0.07 meV), which is consistent with published measurements on thermally annealed NTD Si with similar donor concentrations [10]. The integrated area of a Lorentzian fit to the $2p^{\pm}$ line at 316 cm^{-1} is 15.4 ± 1.0 cm^{-2} for the two athermally treated samples, and 18.5 ± 0.5 cm^{-2} for the thermally annealed sample. Thus we estimate activated donor concentrations of $(6.6 \pm 0.4) \times 10^{14}$ cm^{-3} and $(7.9 \pm 0.2) \times 10^{14}$ cm^{-3} for the athermally and thermally annealed cases, respectively.

Figure 2 shows the temperature dependence of the mobilities and carrier densities in the same two samples. After annealing, a low temperature process was used to attach electrical leads to the corners of the samples for Hall characterization using the Van der Pauw method. Measurements were performed at temperatures between 20 and 300 K and at magnetic fields from 0 to 7 T. Analysis of the results, performed using the Quantitative Mobility Spectrum Analysis (QMSA) method [8], shows the presence of a single electron species whose concentration corresponds to 1.1×10^{15} cm^{-3} activated donors. A fit of the standard freeze-out relation [14] to the electron-concentration vs temperature data implied a donor binding energy of 43 meV, which agreed well with published results for Si:P [15]. The mobility agreed with theoretical predictions for thermally annealed, uncompensated *n*-type silicon [16], as well as with previous experimental results for comparably doped melt-grown Si:P (see Ref. [15]). At <40 K, the athermally annealed samples had a slightly higher mobility, implying that the compensation may be somewhat less than in Ref. [15]. These results also demonstrated that lattice damage was removed to an extent that it has no detectable effect on the mobility.

Four-point probe measurements, with 1-mm spatial resolution, on the athermally annealed samples showed that electrical activation was uniform with no systematic position-dependent variation across either the front or back surfaces of the sample. In particular, resistivity near the slab edges and corners, where shock wave reflections are expected to occur, was not measurably different from resistivities closer to the center of the slab. The *n*-type sheet resistivity of 56 ± 1 ohms/square for the athermally annealed samples compared with an *n*-type sheet resistivity of 130 ohms/square for a thermally annealed NTD slab, *p*-type 1000 ohms/square for an undoped wafer, and an unmeasurably high sheet resistivity for an unannealed NTD sample.

X-ray topographs and rocking curve measurements on unannealed NTD samples showed no differences from bulk Si, indicating that damage in the form of polycrystalline islands was not formed during the NTD process. The measurement does not rule out damage in the form of small regions of amorphous silicon or clusters of vacancies. No residual strain or excess dislocations were introduced by the laser pulse in annealed regions far away from the focal spot. The unit-cell length parameter at 2-mm or more from the focal spot center was 5.430 ± 0.002 Å, a value consistent with that of undamaged silicon. Closer to the focal spot the unit cell parameter increased to ~5.445 Å, indicating that the lattice is under a residual tensile strain of 0.2%–0.3%.

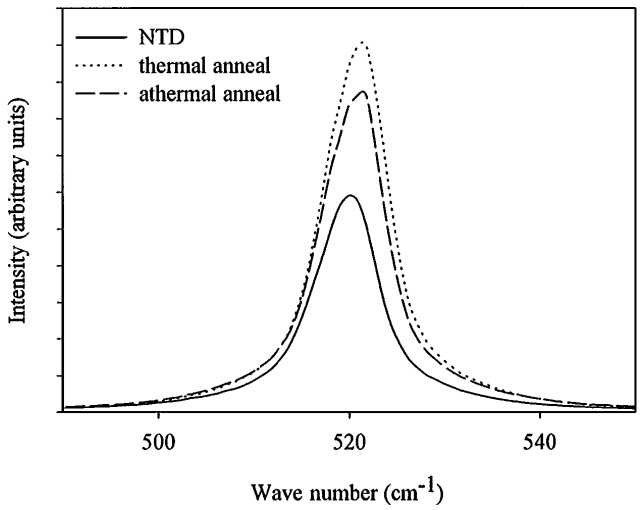

FIG. 3. Raman spectra from NTD Si:P slabs which were unannealed, thermally annealed, and athermally annealed. Undoped Si wafers have Raman spectra very similar to those from thermally annealed samples. The resolution of the measurement is 2 cm^{-1}.

Raman spectroscopy can be a sensitive probe of material crystallinity, particularly in the case of polycrystalline or amorphous silicon [17]. Figure 3 shows Raman spectra for unannealed, thermally annealed, and athermally annealed NTD samples. The thermally annealed sample had a sharp longitudinal optical (LO) phonon mode at 521.0 ± 0.2 cm^{-1}. A most noticeable effect of NTD on this mode was the reduction in its peak intensity by about a factor of 2 everywhere on the front and back of the sample. Correlated with this was a slight redshift of 0.5 ± 1 cm^{-1}. Athermal annealing blueshifted the line back to 521 cm^{-1} and its intensity recovered to within 10% of the thermally annealed sample. X-ray measurements showed no polycrystalline islands or strain that could account for the reduction in Raman intensity and the redshift.

The mechanisms for the absorption of high-intensity laser energy and for the creation and transport of mechanical and thermal energy beyond the illuminated spot are very well known [18–22]. At an irradiance of 3×10^{11} W/cm^2 $\sim$100% of the laser energy is absorbed by a plasma above the slab surface. This plasma, which is very hot ($\sim$200 eV), expands rapidly ($\sim$200 km/s) generating a back-pressure ($\sim$0.2 Mbar) which drives a shock wave into the sample's interior. After traveling a short distance ($\sim$0.5 mm) the shock is weakened by rarefaction waves and by geometrical expansion so that quickly its pressure is drastically reduced (e.g., $\sim 1/1000$ of original strength by 1 cm). Further decrease in pressure is gradual. Before they decay away, the pressure waves and accompanying rarefaction waves reverberate within the sample. In contrast, temperature falls with distance very quickly [23] so than no significant heating occurs outside the illuminated spot.

We conjecture that the athermal annealing in our samples is caused by mechanical energy since that is the only form of energy that could have traveled so far ($\sim$1 cm) beyond the spot where the laser energy was deposited. The mechanism cannot involve bulk heating because the laser does not have sufficient energy to heat the entire sample significantly. Temperatures capable of annealing, i.e., 900 °C, exist only near the edge of the illuminated spot. This is consistent with our observation that melting, which occurs at temperatures greater than 1414 °C, exists only within the immediate neighborhood of the focal spot. Heating by visible or x-ray radiation from the laser-heated plasma cannot play a role since the back of the slab, which was shielded from this radiation, was annealed as effectively as the front. Similarly, the laser's 1.06-μm radiation cannot be responsible because almost all of the laser energy is absorbed by the plasma (formed at $\sim 10^8$ W/cm^2) above the slab surface [24]. Thus mechanical energy is the most plausible candidate to explain the observed activation.

In summary, we have annealed NTD silicon slabs without the direct application of heat. Details of the process such as thresholds, etc., need to be determined, and a comprehensive theoretical understanding is yet to be developed. It remains to be shown whether the process can anneal semiconductors other than NTD silicon, whether its reproducibility can be improved, and whether it will be effective on industrial-scale wafers.

We thank Mr. Kirk Evans, Mr. Rayvon Burris, Mr. Levi Daniels, and Mr. Nicholas Nocerino for their able technical assistance, and Dr. Richard Singer, Dr. Larry Larson, Dr. Mike Bell, Dr. Richard Hubbard, and Dr. Benjamin V. Shanabrook for their sound advice and assistance. Shock characteristics at distances larger than 1 mm are based on simulations performed by Dr. B. Stellingwerf and Dr. C. Wingate at LANL. Using the SPHINX SPH code they modeled shocks and rarefaction waves inside a 1-mm thick, 10-cm diameter aluminum disk irradiated at its center by a 4-joule pulse focused to a 1-mm spot. This project was supported by The Electronics Technology Office of The Defense Advanced Research Projects Agency.

[1] J. P. De Souza and D. K. Sadana, in *Handbook on Semiconductors*, edited by S. Mahajan (Elsevier, Amsterdam, 1994), Vol. 3, Chap. 27.

[2] J. C. Hsieh, Y. K. Fang, C. W. Chen, N. S. Tsai, M. S. Lin, and F. C. Tseng, IEEE Trans. Electron Devices **41**, 692 (1994).

[3] R. Liu, C. Y. Lu, J. J. Sung, C. S. Pai, and N. S. Tsai, Solid-State Electron. **38**, 1473 (1995).

[4] *Semiconductors and Semimetals*, edited by R. F. Wood, C. W. White, and R. T. Young (Academic, New York, 1984), Vol. 23.

[5] D. Alexiev, *Neutron Transmutation Doping of Silicon for the Production of Radiation Detectors* (Lucas, Sydney, 1987).
[6] J. W. Cleland, *Radiation Damage in Solids* (Academic, New York, 1962); C. Chang, *Gamma Radiation Damage in Silicon*, thesis, University of Missouri–Columbia, 1993.
[7] R. T. Young, J. W. Cleland, R. F. Wood, and M. M. Abraham, J. Appl. Phys. **49**, 4752 (1978).
[8] J. R. Meyer, C. A. Hoffman, F. J. Bartoli, D. J. Arnold, S. Sivananthan, and J. P. Faurie, Semicond. Sci. Technol. **8**, 805 (1993).
[9] J. R. Meyer, C. A. Hoffman, F. J. Bartoli, J. Antoszewski, L. Faraone, S. P. Tobin, P. W. Norton, C. K. Ard, D. J. Reese, L. Colombo, and P. K. Liao, J. Electron. Mater. (to be published).
[10] C. Jagganath, C. W. Grabowski, and A. K. Ramdas, Phys. Rev. B **23**, 2082 (1981).
[11] S. B. Qadry and J. H. Dinan, Appl. Phys. Lett. **47**, 1066 (1985).
[12] S. B. Qadry, M. Fatemi, and J. H. Dinan, Appl. Phys. Lett. **48**, 239 (1986).
[13] M. H. Brodsky, in *Light Scattering in Solids I,* edited by M. Cardona, Topics in Applied Physics Vol. 8 (Springer-Verlag, New York, 1983).
[14] J. S. Blakemore, *Semiconductor Statistics* (Pergamon, New York, 1962), Chap. 3.
[15] P. Norton, T. Braggins, and H. Levinstein, Phys. Rev. B **8**, 5632 (1973).
[16] L. E. Kay and T. W. Tang, J. Appl. Phys. **70**, 1475 (1991).
[17] H. Richter, Z. P. Wang, and L. Ley, Solid State Commun. **39**, 625 (1981).
[18] B. H. Ripin *et al.,* Phys. Fluids **23**, 1012 (1980).
[19] J. Grun, R. Decoste, B. H. Ripin, and J. Gardner, Appl. Phys. Lett. **39**, 545 (1981).
[20] B. Meyer and G. Thiell, Phys. Fluids **27**, 302 (1983).
[21] J. Grun, R. Stellingwerf, and B. H. Ripin, Phys. Fluids **29**, 3390 (1986).
[22] R. J. Trainor and Y. T. Lee, Phys. Fluids **25**, 1898 (1982).
[23] L. D. Landau and E. M. Lifshitz, *Fluid Mechanics* (Butterworth and Heinemann, Oxford, 1995), Chap. 5.
[24] Yu. A. Bykovskii, N. N. Degtyarenko, V. F. Elesin, Yu. P. Kozyrev, and S. M. Sil'nov, Soviet Phys. JETP **33**, 706 (1971), and references therein.